DEVELOPMENT OF A METHOD TO REALIZE A UNIFORM SOUND FIELD IN THREE-DIMENSIONAL SPACES BASED ON THE RAY-TRACING ALGORITHM

Yigang Lu [*1] and Hengling Song [†1]
[1]School of Architecture, South China University of Technology, Guangzhou, China

Résumé

Dans la présente étude, une méthode de cartographie des mouvements de rayons dans les espaces géométriques tridimensionnels a été établie théoriquement en utilisant un algorithme de radiosité (*ray-tracing*). Les chemins le long desquels se propage le rayon acoustique dans des espaces clos rectangulaires et concaves sont décrits selon l'algorithme de radiosité. La localiation et la direction du rayon acoustique à des points arbitraires sur les chemins ont été explorés. Les plus grands exposants de Lyapunov (PGEL) des systèmes de rayons dans les espaces rectangulaires et concaves ont été déterminés en utilisant l'algorithme de Wolf selon les points sur les chemins de propagation avec une longueur égale dans la série chronologique. Une nouvelle géométrie chaotique concave est produite avec un PGEL positif. Les PGEL de la dynamique de rayon entre les deux espaces géométriques ont été comparés et les résultats indiquaient que le rayon se déplace de manière régulière dans l'espace rectangulaire avec un PGEL de 0 tandis que le rayon adopte un comportement chaotique dans l'espace concave avec un PGEL positif. Les champs acoustiques dans chacun de ces espaces ont été décrits en appliquant le chaos du rayon à l'acoustique des bâtiments. La diffusion acoustique a été évaluée selon l'uniformité des niveaux de pression acoustique à différentes positions dans le champ acoustique en utilisant un logiciel d'acoustique de la salle Odeon. Les résultats ont démontré que le modèle proposé a le potentiel de simuler la dynamique chaotique des rayons acoustiques dans les espaces clos.

Mots clefs : diffusion, ray-tracing, radiosité, plus grand exposant de Lyapunov, algorithme de Wolf, acoustique des salles

Abstract

In this study, a method of mapping ray motions in three-dimensional geometrical spaces was theoretically established using the ray-tracing algorithm. The paths along which the acoustic ray propagates in enclosed rectangular and concave spaces are described according to the ray-tracing algorithm. The location and the direction of the acoustic ray at arbitrary points on the paths were explored. The largest Lyapunov exponents (LLEs) of the ray systems in the rectangular and concave spaces were determined using the Wolf algorithm based on the points on the propagation paths with equal length in the time series. A new chaotic concave geometry is produced with a positive LLE. The LLEs of ray dynamics between the two geometrical spaces were compared and the results showed that the ray moves in a regular fashion in the rectangular space with an LLE of 0 whereas the ray exhibits chaotic behavior in the concave space with a positive LLE. The acoustic fields in both of these spaces in were described by applying ray chaos to the building acoustics. The acoustic diffusion was evaluated based on the uniformity of the sound pressure levels at different positions in the sound field using Odeon room acoustics software. The results showed that the proposed model has the potential to simulate chaotic dynamics of acoustic rays in enclosed spaces.

Keywords: diffusion, ray-tracing algorithm, largest Lyapunov exponent, Wolf algorithm, room acoustics

1 Introduction

Particle billiard theory is originally used in the electromagnetic field [1, 2] and in quantum mechanics studies [3–5]. However, in room acoustics, the scenario in which the sound rays bounce back and forth in an enclosed space can be analyzed by establishing the sound ray model. Tracking acoustic arrays is crucial for ocean acoustics applications such as underwater acoustic communication and ocean acoustic tomography. Li et al. [6], Brown et al. [7], and Makarov et al. [8] used the ray chaos model to investigate the effects of sound velocity on the system dynamics behavior in underwater acoustics. The results showed that the acoustic ray system was randomly interfered underwater because of the characteristics of the inhomogeneous seawater medium. Studies on the effects of random disturbance on the characteristics of the acoustic ray system characteristics showed that the acoustic ray motions changed from regular to irregular or the original irregular motions of the acoustic rays were intensified when a random disturbance was introduced into the system and the intensity of the random disturbance was increased. In the absence of reflections underwater, the increased disturbance of the internal waves on the sound velocity resulted in a system with a positive Lyapunov exponent. This increased the chaotic motion of the acoustic rays and expanded the chaotic region [9]. Similar to the results obtained for

[*] phyiglu@scut.edu.cn
[†] shm3214974@hotmail.com

underwater acoustics, Kawabe et al. [10] found that perturbations in the sound velocity resulted in a chaotic acoustic ray propagation due to the temperature fluctuations caused by the inhomogeneous medium in the room. For example, for a two-dimensional space with an inhomogeneous medium, there were slight deviations in the acoustic ray trajectories such that the acoustic rays did not travel in a straight line because of perturbations. The acoustic ray trajectory was curved when there were temperature fluctuations in the medium. Ray chaos was observed in the domain when perturbations due to the inhomogeneity of the medium were considered in the analysis. However, for a homogeneous medium, the non-interacting rays would always propagate along a straight trajectory between the boundaries of the domain. According to the billiard theory, the chaotic behavior of acoustic rays is closely related to the geometry of the enclosed space. Koyanagi et al. [11] used the square well potential model to simulate the acoustic ray motions in a room where the absorption was uniformly distributed along the boundaries and the results showed that the square well potential model can be used to determine the reverberation time in a two-dimensional enclosed space. They computed the largest Lyapunov exponents (LLEs) and they believed that reverberation of the sound field was related to the ray chaos of the billiards in the polygons with smooth convex walls. Yu and Zhang [12, 13] used 13 acoustic ray equations to describe the acoustic ray motions in a two-dimensional semicircle stadium model and computed the Lyapunov spectrum of the ray systems using the classic Wolf algorithm. They obtained the power law of the Lyapunov exponents used in architectural acoustics in order to describe the characteristics of acoustic defects such as diffusion, flutter echoes, and acoustic focusing. Most of the studies published to date are focused on two-dimensional systems because the simplest form of classical chaos is two-dimensional. However, a three-dimensional system is a more accurate representation of the real-world system and it has more practical significance in architectural acoustics. Hence, this work is focused on investigating acoustic ray chaos in a three-dimensional enclosed space based on a two-dimensional enclosed space.

The remainder of this paper is organized as follows. The ray-tracing algorithms used to track the trajectories of acoustic rays in the geometrical space are presented in Section 2. The LLEs of ray systems in the rectangular and concave enclosed spaces were calculated and presented in Section 3, in which the chaotic characteristics for the concave geometry are derived. The ray systems are then used for building acoustics and the results are validated using Odeon room acoustics software, as presented in Section 4. Finally, the conclusions drawn based on the findings of this study are presented in Section 5 and the significance of the method proposed in this work is highlighted.

2 Method

2.1 Ray-tracing algorithm

The points in the time series used to determine the LLEs are extracted from the reflection paths in a three-dimensional geometrical space using the random ray-tracing algorithm. The ray moves in a straight trajectory with an initial direction from a source in the geometrical space and the ray then changes its direction when it encounters a surface. In this algorithm, it is assumed that only specular reflections occur and therefore, the angle of reflection is equal to the angle of incidence at each point on the surface. Figure 1 shows the ray reflections on the rigid smooth boundary of a geometrical space.

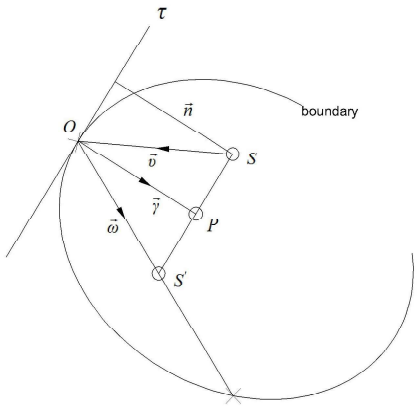

Figure 1: Specular reflections on the rigid smooth boundary of a geometrical space.

It is assumed that the acoustic ray moves in the domain (which is determined by the geometrical space) depending on the reflections at the boundaries:

$$f_i(x,y,z)=0,\ i\in Z^d, d\geq 1 \tag{1}$$

The launching ray $\overline{SO}$ exerted by the source S is given by:

$$\begin{cases} x = x_0 + at \\ y = y_0 + bt \\ z = z_0 + ct \end{cases},\ t\in R_+ \tag{2}$$

Where $S(x_0, y_0, z_0)$ represents the coordinates of the source and $\vec{v}=(a,b,c)$ represents the directional vector of the incident ray, which is not normal to the boundary. A singularity will occur if the directional vector is normal to the boundary.

The reflection point, $O(x_0+at_{min}, y_0+bt_{min}, z_0+ct_{min})$ is determined by substituting Eq. (2) into Eq. (1), where the line intersects the surface of the boundary:

$$f_i(x_0+at_{min}, y_0+bt_{min}, z_0+ct_{min})=0 \tag{3}$$

Here, the subscript "*min*" stands for minimum parameter "*t*", which is required for the intersection.

The normal vector across the reflection point is expressed as:

$$\vec{n} = \left(\frac{\partial f(x_{min}, y_{min}, z_{min})}{\partial x}, \frac{\partial f(x_{min}, y_{min}, z_{min})}{\partial y}, \frac{\partial f(x_{min}, y_{min}, z_{min})}{\partial z} \right) \quad (4)$$

The normal vector $\vec{\gamma}$ is determined from the projection method, as follows:

$$\vec{\gamma} = -\frac{\vec{v} \bullet \vec{n}}{|\vec{n}|^2} \vec{n} \quad (5)$$

Hence, the direction of the reflected ray $\overline{OS'}$ is confined by $\vec{\omega} = \vec{v} + 2\vec{\gamma}$.

The reflection path in a three-dimensional enclosed space is traced by successive iterations of the new reflection points and directions of the reflected rays.

The following cases need to be avoided because they result in singularities:

- The acoustic ray hits into a corner;
- The acoustic ray is normal to the boundary surface;
- The reflected acoustic rays are all on the same plane.

The acoustic ray will lose its consistency in the first and second cases whereas the acoustic ray has consistency in the third case, but it will not reflect on all surfaces.

Based on the above mapping procedure, the position and direction of the acoustic ray can be obtained at any arbitrary point on the propagation paths in a three-dimensional geometrical space, even for complex geometries. The time series used to compute the LLEs is derived from the points on the propagation paths. Two geometries (rectangular and concave enclosed spaces) have been widely studied in architectural acoustics. In this study, the LLEs were introduced to the ray systems in rectangular and concave enclosed spaces. Previous studies have shown that the propagation of an acoustic ray in an enclosed space is analogous to the particle trajectory in a billiard system within a high-frequency limit [10, 14]. Figure 2 shows the acoustic ray motions in the rectangular and concave enclosed spaces.

The ray-tracing algorithms were used to determine the acoustic ray motions and derive the time series in order to perform the Lyapunov exponent analysis. In the numerical simulations, the incident ray is launched with an initial direction from a source in the geometrical space. Many simulation runs were performed and it was found that changes in the source location and direction of the launching ray did not affect the LLE values. Because the continuity of the reflected rays is guaranteed, the method can be used to simulate motions of acoustic rays reflecting off a surface from an arbitrarily located source in various geometrical spaces. The method can also be used to simulate ray motions irrespective of the launching direction, provided that the acoustic ray is not perpendicular to the boundary surface.

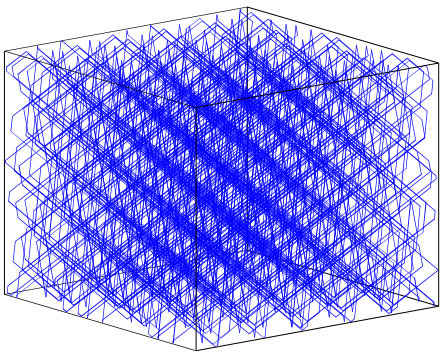

(a)

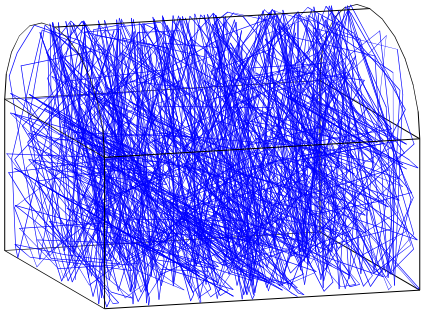

(b)

Figure 2: Ray motions in the (a) rectangular and (b) concave enclosed spaces.

With the exception of the three singularities mentioned previously, it can be seen that the acoustic ray is launched from the source in the geometrical space in the direction indicated by the directional vector. It is possible to derive the directional vectors for the rectangular and concave geometries by tracing the ray propagation.

The ray has four ($2^2 = 4$) and eight ($2^3 = 8$) possible direction values for the two-dimensional and three-dimensional rectangular geometries, respectively. The base number "2" refers to the reverse directions in which the ray rebounds whereas the exponent number refers to the dimension of the space. For an initial directional vector (*a*, *b*, *c*), there are eight possible directions for the acoustic ray in the rectangular geometry: (*a*, *b*, *c*), (*a*, -*b*, -*c*), (*a*, -*b*, *c*), (*a*, *b*, -*c*), (-*a*, -*b*, -*c*), (-*a*, -*b*, *c*), (-*a*, *b*, -*c*), and (-*a*, *b*, -*c*). However, there is a large number of directions for the acoustic ray in the concave geometry. MATLAB computer aided engineering software (Release 2012b, MathWorks, Inc., USA) was used for the numerical simulations. The ray was launched from the source point (1, 1, 1) in the direction of $\left(1, \tan\alpha, \tan\alpha * \sqrt{1 + (\tan\alpha)^2}\right)$, where $\alpha = 75°$. This means that the ray is inclined at angle of 75° from the vertical planes *X*-*Y* and *X*-*Z* in the geometrical space. The length, width, and height of the rectangular space are 6.80, 6.62, and 5.10, respectively. The length, width, height, and radius of the concave space are 6.80, 6.62, 3.21, and 3.00,

respectively. The elements of each directional vector refer to the ray direction from the point of origin to the vector point. The large number of directional vectors creates a vector field, which gives the directional vector of the acoustic ray at every point. Figure 3 shows the projection of the directional vectors onto the *X*-*Z* and *Y*-*Z* planes (denoted by the blue asterisks), which is obtained by substituting the *y* or *x*-coordinate of the directional vectors with 0. The acoustic ray reflects 10000 times in the concave space. The ray propagates in eight directions in the rectangular space whereas the reflected ray in the concave space propagates in different directions, where the directional vectors projected onto the *X*-*Y* and *X*-*Z* planes follow an angular distribution (Figure 3(a)) whereas the directional vectors projected onto the *Y*-*Z* plane follow a circular distribution (Figure 3(b)). There is an exponential proliferation of acoustic rays in the concave space due to the sensitivity of the ray trajectories to the initial conditions for a chaotic system.

By applying this ray-tracing model in room acoustics, the ray will propagate repeatedly in a small number of directions in the rectangular space, which produces acoustic effects because the sound waves are reflected back and forth between the parallel reflective surfaces. This phenomenon is known as "flutter echo" in room acoustics, in which strong points are generated at locations where the sound energy is concentrated in one direction.

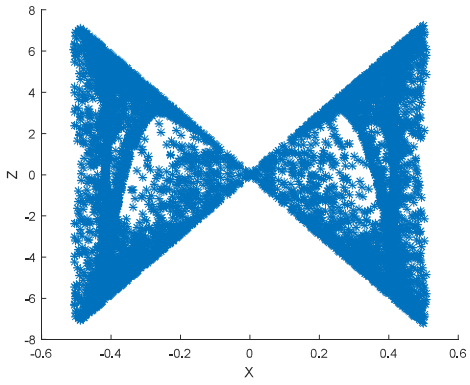

(a)

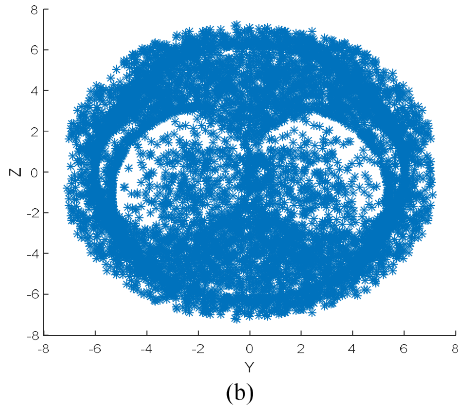

(b)

Figure 3: (a) Angular distribution of the directional vectors projected onto the *X*-*Z* plane and (b) circular distribution of the directional vectors projected on the *Y*-*Z* plane (b) in the concave space.

In contrast, the concentration of sound energy in one direction is reduced and the uniformity of the sound field is improved in a concave space because the ray propagates from various possible directions in the *Y*-*Z* plane.

Figure 4 shows the distributions of *Z*-values taken from 150 points on the propagation paths of equal length for the rectangular and concave spaces. In this case, equal length means that the ray is divided into length intervals (*dL*) of equal time *t* for a specific sound propagation velocity *c*. The *Z*-values were plotted against the number of points *N* for the ray trajectories with multiple reflections. The *Z*-value distributions clearly show the time series of the ray trajectories in the rectangular and concave enclosed spaces.

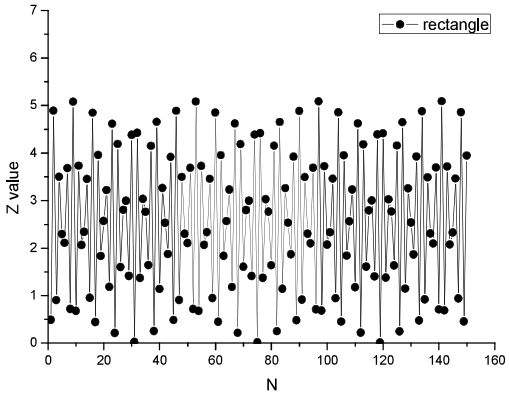

(a)

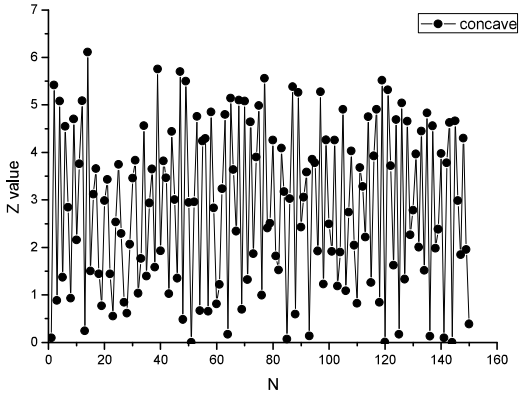

(b)

Figure 4: Distributions of *Z*-values taken from 150 points on the ray propagation paths of equal length for the (a) rectangular and (b) concave enclosed spaces.

2.2 Determination of the LLEs

The Lyapunov exponent is a quantity that characterizes the rate of separation of infinitesimally close ray trajectories. In other words, the ray separation is sensitive to the initial conditions of the system. The system is considered chaotic if at least one Lyapunov exponent is positive [15]. The sensitivity of the ray separation to the initial conditions of the chaotic system makes it possible to investigate the diffusive behavior of rays in various enclosed spaces.

Assuming that there are two (usually the nearest) neighboring points in the phase space at time 0 and time t, the distances of the points in the i^{th} direction are denoted as $\|\delta x_i(0)\|$ and $\|\delta x_i(t)\|$, respectively. The Lyapunov exponent is then defined by the average growth rate λ_i of the initial distance, which is given by:

$$\lambda_i = \lim_{t\to\infty} \frac{1}{t} \log_2 \frac{\|\delta x_i(t)\|}{\|\delta x_i(0)\|} \tag{6}$$

The set $\{\lambda_1, \cdots, \lambda_{max}\}$ is called the Lyapunov spectrum. Although the full Lyapunov spectrum can provide detailed information on the dynamic behavior of the system, it is not practical to compute the full Lyapunov spectrum because of the lengthy computational time. For this reason, LLEs are computed to validate a chaotic system rather than the complete Lyapunov exponents. In this study, the Wolf algorithm was used to determine the LLEs of the ray systems in the rectangular and concave spaces based on the time series.

The Wolf algorithm estimates the LLEs from a finite number of time series values by keeping the track of the exponentially divergent adjoining trajectories, as shown in Figure 5. The time series data for a single coordinate of the chaotic system (measured at equal time intervals) was considered in this study and the degree of the trajectory divergence was evaluated at regular intervals. There are five steps involved to determine the LLEs. First, select the point closest to the initial point on the fiducial trajectory at time t_0. The distance between both of these points is denoted as $L(t_0)$. Second, let $L'(t_1)$ denote the distance between two points on the fiducial trajectory and neighboring trajectory at a later time t_1. Next, compute the exponential ratio of $L'(t_1)$ to $L(t_0)$. Third, select the closest point at t_1 such that θ_1 is minimum and measure the distance $L(t_1)$. Fourth, repeat the second step at t_2 after time Δt and then compute the exponential ratio. Fifth, repeat the above procedure M times and compute the average exponential ratio. The LLE is defined as:

$$LLE = \frac{1}{M\Delta t} \sum_{k=1}^{M} \log_2 \frac{L'(t_k)}{L(t_{k-1})} \tag{7}$$

Where $\Delta t = t_k - t_{k-1}$ and M is the number of iterations. The parameters $L'(t_k)$ and $L(t_{k-1})$ are calculated from the Euclidean distance.

The LLEs for the rectangular and concave spaces were determined based on the time series points on the trajectory with equal length intervals dL, where the values on the z-coordinate are taken as its own series, as shown in Figure 6.

It can be seen that the LLE values are ~0 and ~0.3 for the rectangular and concave spaces, respectively. It is evident that there is a positive Lyapunov exponent for the ray system in the concave geometry, which indicates that chaos has truly developed.

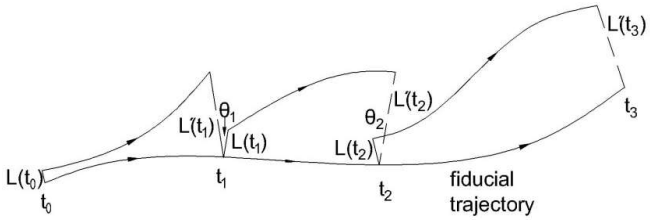

Figure 5: Procedure used to estimate the LLEs from the experimental data.

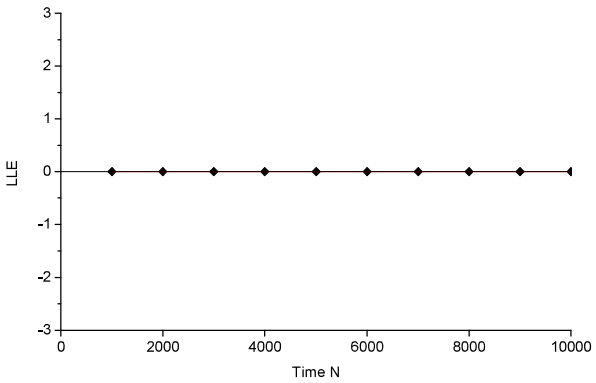

(a)

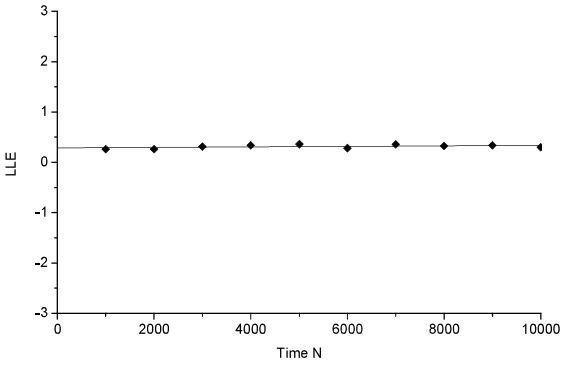

(b)

Figure 6: LLEs of the ray systems in the (a) rectangular and (b) concave enclosed spaces.

In contrast, an LLE value of 0 indicates that two nearby rays will not separate exponentially with respect to time. In other words, the ray moves in a regular fashion in the rectangular space. Nevertheless, when the LLE value is positive, the ray motion shows chaotic characteristics, such as that in the concave space. In room acoustics, a ray system with a positive Lyapunov exponent indicates the ray trajectories are sensitive to the initial conditions of the system and the rays may be diffuse [16].

3 Simulations of room acoustics using Odeon software

In room acoustics, sounds may propagate as rays at high frequencies. Ray acoustics is deemed to be a part of the ray moments in the geometrical space and therefore, it is possible to account for ray chaotic behavior in building acoustics. Empirically, a perfectly diffused enclosed space is

defined as one in which there are equal levels of sound energy at all positions and the sound energy flows equally in all directions upon excitation by a source. The definition of a diffuse field is probably adequate from a conceptual standpoint, but it does not provide much information from an operational viewpoint. At present, there are no practical direct metrics for this concept and there are no reliable methods to determine the diffusion levels in an enclosed space. Hence, it is not possible to state the diffusion level required for a given application. For this reason, most researchers attempt to create a test environment that is representative of an ideal physical scenario using mathematical models that are developed based on the current knowledge on ray theories. The diffusion levels of an enclosed space can be evaluated using either one of the following methods: (1) spatial uniformity of pressure method, which involves measuring the spatial variations of the sound pressure levels (SPLs), (2) cross-correlation analysis method, which involves measuring the degree of correlation between the sound pressure measurements at different microphone positions, (3) acoustic wattmeter method, which involves measuring the vector energy flow, (4) directional diffusion method, which involves measuring the sound levels in different directions using a directional microphone, and (5) multifractal method, which involves assessing the diffusion levels using a singularity spectrum corresponding to a monofractal signal [17–20]. At present, there are limited means to quantify the diffusion levels in an enclosed space. This work is focused on exploring the diffusion levels of sound field based on the uniformity of the SPLs in the enclosed space.

It has been shown [21] that the source directivity directly affects the uniformity of the sound field. In reality, the sources used in auditoriums, especially those produced by electro-acoustical instruments, are usually directional. Thus, studies on the uniformity of room acoustics with a directional source are of great significance to architectural researchers and designers during the early stages of design.

The acoustic diffusion was evaluated using Odeon 12.2 room acoustics software, which is a software typically used to simulate room acoustics with complex geometries [22] based on the image source and ray-tracing methods. In order to approximate the specular reflections on the rigid walls, the absorption and scatter coefficients were assigned a value of 0.01 and 0, respectively. Both the absorption and scatter coefficients were assumed to be uniformly distributed over all surfaces in the enclosed space. A directional source was used for the simulations. Because a directional source was used in the model (where the directivity of the source is at an angle), the sound transmission is more complete due to the rays coming from various directions compared to a source with stronger directivity. Even though the default line number provided in the Odeon software was 2000, many studies have shown that the directivity of the source is influenced by a line number up to 500. Thus, a suitable line number needs to be chosen for the simulations when the directivity of the source is considered. The line number should be within a range of 25–100 because the directivity of the source is at an angle. It is found in this study that a higher line number reduces the effect of directivity whereas a line number within a range of 100–500 leads to obscure results. In contrast, the directivity of the source does not affect the diffusion of room acoustics when the line number is greater than 500. Increasing the line number may reduce dependency of the acoustic performance on the geometry of the enclosed space, but this comes at the expense of a loss of directivity. Even though increasing the line number will improve the ray distribution in both rectangular and concave enclosed spaces, the line number should be limited to a maximum of 500 to ensure that the directivity of the source is not entirely lost.

For the simulations, the line number required is available within the range in which the directivity of the source is valid. In this study, the line number and impulse response length were set at 25 lines and 5000 ms, respectively. It is found that temperature and humidity will not significantly affect the results, indicating that the sound ray still propagates in a straight trajectory within a normal range at high frequencies. Information of the directivity of the loudspeaker is provided by the CLF Group [23]. Because the software is based on geometrical acoustics, only the sample directivity balloons for selected octave bands (1000, 2000, 4000, and 8000 Hz) were chosen for this work, as shown in Figure 7.

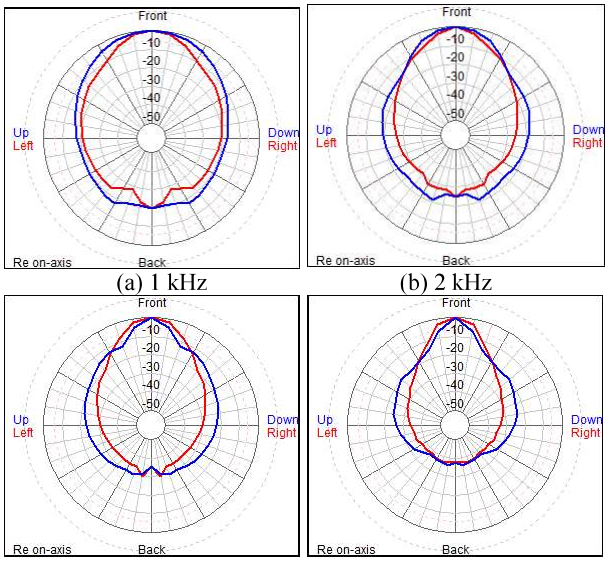

Figure 7: Directivity patterns of the "DNH-Tunnel-500" source at different frequencies [17]. The sample directivity balloons for the loudspeakers were used for validation, with the axis pointing to the left as "front" in three dimensions for the following octave bands: (a) 1 kHz, (b) 2 kHz, (c) 4 kHz, and (d) 8 kHz.

The SPLs at 20 receiver positions obtained from the simulations were compared to evaluate the status of the sound field. Figure 8 shows the top view and side view of the spatial distribution of the source and receivers. The source is positioned at one corner of the enclosed space and the receivers are positioned in a grid, as indicated by the numbered circles. These receivers are considered to occupy the whole space. The distances between the source,

receivers, and surfaces comply with the requirements of the ISO 3382 standard. The positions of the source and receivers in the rectangular and concave enclosed spaces are summarized in Table 1.

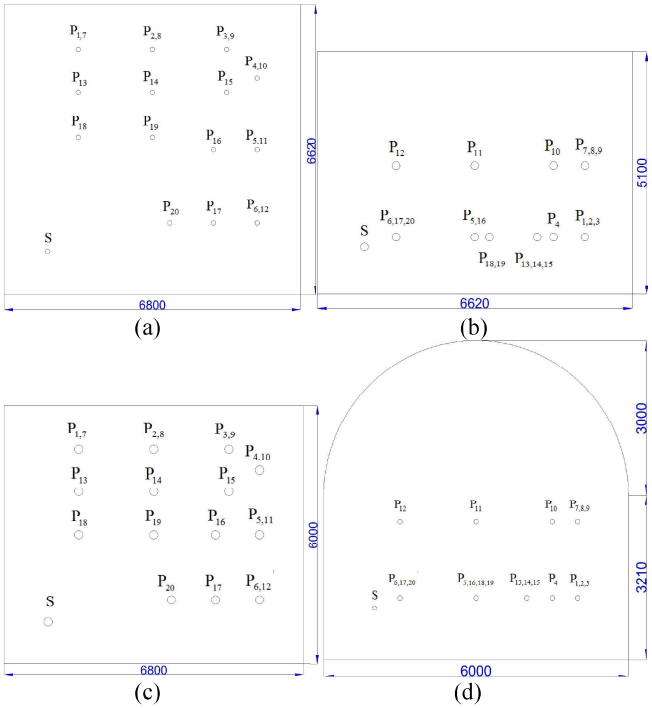

Figure 8: (a) Horizontal and (b) vertical layouts of the source and receivers in the rectangular space (length = 6800 mm, width = 6620 mm, height = 5100 mm); (c) Horizontal and (d) vertical layouts of the source and receivers in the concave space (length = 6800 mm, width = 6620 mm, height = 3210 mm, radius = 3000 mm).

4 Results and discussion

The differences of the SPLs between 20 receiver points were compared based on the range and variance, as shown in Table 2. The range represents the difference between the highest and lowest SPLs while the variance indicates the fluctuations of the SPLs in the sound field. Table 2 shows the uniformity of the sound field under excitation of the "DNH-Tunnel-500" source.

It can be seen from Table 2 that the receivers located at sites in front of the source have relatively higher SPLs, regardless whether the enclosed space is rectangular or concave. The range and variance of the SPLs are smaller for the concave space compared with those for the rectangular space for the frequency bands investigated in this work. The range is larger at higher frequency bands. The sound energy distribution is more homogeneous in the concave space because of the chaotic behavior of the acoustic rays, which is consistent with the theoretical results of ray chaos. Because the ray system in the concave space has a positive LLE, the ray separation is sensitive to the initial conditions of the chaotic system. Therefore, the ray distribution has better diffusion characteristics in a concave space.

Table 1: Positions of the source and receivers in the rectangular and concave enclosed spaces.

	Rectangle	Concave		Rectangle	Concave
S	(1,1,1)	(1,1,1)	S	(1,1,1)	(1,1,1)
P_1	(1.70,5.62,1.20)	(1.70,5.00,1.20)	P_{11}	(5.80,3.31,2.70)	(5.80,3.00,2.70)
P_2	(3.40,5.62,1.20)	(3.40,5.00,1.20)	P_{12}	(5.80,1.66,2.70)	(5.80,1.50,2.70)
P_3	(5.10.5.62,1.20)	(5.10.5.00,1.20)	P_{13}	(1.70,4.62,1.20)	(1.70,4.00,1.20)
P_4	(5.80,4.96,1.20)	(5.80,4.50,1.20)	P_{14}	(3.40,4.62,1.20)	(3.40,4.00,1.20)
P_5	(5.80,3.31,1.20)	(5.80,3.00,1.20)	P_{15}	(5.10,4.62,1.20)	(5.10,4.00,1.20)
P_6	(5.80,1.66,1.20)	(5.80,1.50,1.20)	P_{16}	(4.80,3.31,1.20)	(4.80,3.00,1.20)
P_7	(1.70,5.62,2.70)	(1.70,5.00,2.70)	P_{17}	(4.80,1.66,1.20)	(4.80,1.50,1.20)
P_8	(3.40,5.62,2.70)	(3.40,5.00,2.70)	P_{18}	(1.70,3.62,1.20)	(1.70,3.00,1.20)
P_9	(5.10,5.62,2.70)	(5.10,5.00,2.70)	P_{19}	(3.40,3.62,1.20)	(3.40,3.00,1.20)
P_{10}	(5.80,4.96,2.70)	(5.80,4.50,2.70)	P_{20}	(3.80,1.66,1.20)	(3.80,1.50,1.20)

Table 2: Uniformity of the sound field under excitation of the "DNH-Tunnel-500" source.

	1 kHz	2 kHz	4 kHz	8 kHz
	Rectangle / Concave	Rectangle / Concave	Rectangle / Concave	Rectangle / Concave
1	108.6/108.5	102.8/103.4	88.3/89.2	76.3/77.1
2	108.7/109.2	103.1/104.4	88.8/90.4	76.8/78.5
3	109.2/108.6	103.9/103.7	89.9/89.7	78.0/77.7
4	108.9/109.4	103.8/104.4	89.9/90.2	77.9/78.1
5	109.3/109.7	104.1/104.5	89.9/90.2	77.8/78.0
6	111.1/109.8	106.5/104.4	92.4/89.9	80.2/77.7
7	108.5/109.3	102.6/104.5	88.1/90.4	76.0/78.3
8	108.6/109.5	103.1/104.8	88.8/90.8	76.8/78.6
9	108.7/109.4	103.4/104.7	89.4/90.6	77.4/78.5
10	108.7/109.1	103.6/104.2	89.6/90.2	77.6/78.1
11	109.2/109.2	104.2/103.9	90.1/89.6	78.0/77.5
12	110.3/109.6	105.7/104.3	91.6/89.9	79.4/77.8
13	108.6/109.6	103.3/104.5	89.2/90.3	77.1/78.2
14	109.0/109.9	103.7/104.9	89.6/90.8	77.5/78.7
15	108.8/109.9	103.6/104.9	89.6/90.8	77.5/78.6
16	109.5/109.4	104.3/104.2	90.2/90.0	78.1/77.8
17	111.1/109.9	106.5/104.7	92.5/90.4	80.3/78.2
18	109.0/109.2	104.0/104.1	90.0/89.9	77.9/77.8
19	109.2/109.3	104.2/104.2	90.2/90.0	78.1/77.8
20	111.2/109.4	106.7/104.3	92.7/90.0	80.5/77.9
Range	2.7/1.4	4.1/1.5	4.6/1.6	4.5/1.6
Variance	0.7862/0.1457	1.5110/0.1468	1.7267/0.1760	1.5783/0.172

For an enclosed space with homogeneous medium, the ray motions are determined by the geometry of the space and the characteristics of the sound field are determined by the ray motions. In this work, the ray distribution is more diffusive in a concave space compared to that in a three-

dimensional rectangular space. In addition, the sound field is more uniform in a concave space compared to that in a rectangular space, as shown in Table 2.

In this study, the uniformity of the sound field is focused on the audience area, which is typically the lower and middle section of the room. Hence, it can be deduced that chaos theory is more valid to describe the sound ray mechanism. There are two types of mechanism for chaotic systems [24]: (1) the Sinai billiards (dispersion mechanism), where the dispersing boundary elements in the nearby trajectories diverge upon scattering and the consecutive collisions with the dispersing elements result in higher divergence and (2) Bunimovich stadium billiards (defocusing mechanism), where the nearby trajectories converge after a collision with the focusing boundary elements. The trajectories only begin to diverge after they pass through the focusing point. Provided that the free flight is sufficiently long (including reflections at the neutral boundary elements), the focusing may be overcompensated by divergence, which results in defocusing. It is worth noting that a long free flight is required for weak focusing before defocusing. The sound field is more uniform in a concave space because of the defocusing effects. A positive LLE indicates that separation of the acoustic rays is sensitive to the initial conditions of the chaotic system, which results in a higher uniformity of the sound field in the enclosed space.

It is also evident that the difference in the uniformity of the sound field is higher for intermediate and high frequency bands, regardless whether the enclosed space is rectangular or concave. This indicates that the method proposed in this work is suitable to analyze geometrical acoustics. Ray chaos theory provides a new perspective on the analysis of geometrical acoustics. The sound energy density distribution is more uniform if the acoustic rays exhibit chaotic characteristics. In this study, simulations were performed for different acoustic source ("Danley Sound Labs-SH-25") with a different directivity. Similar results were obtained for this case, as shown in the appendix.

5 Conclusions

In this study, the kinetic behaviors of ray systems in rectangular and concave enclosed spaces were described based on LLEs. A new concave geometry with chaotic ray system was introduced by computing the LLEs of the ray system. By converting the points on the ray trajectories into a time series, the LLEs of the ray systems in three-dimensional spaces were successfully determined without the need for a kinetic equation. The Lyapunov exponent was found to be positive for the concave space, which confirms the chaotic behavior of the ray system in this geometry. A ray system with a positive LLE indicates that the rays behave in an ergodic manner whereas a ray system with an LLE of 0 indicates that the ray motions are regular. According to the ray chaos theory, the rays in a chaotic system are sensitive to the initial conditions of room acoustics, which makes it possible to obtain a uniform sound energy density distribution as in the case of the concave space. Owing to the chaotic characteristics in the concave space, there are less fluctuations of the SPLs in this space compared with that in the rectangular space. The results indicate that the method can be used to assess the acoustic performance of a geometrical space with homogeneous medium based on the dynamics of the acoustic rays.

The method presented in this paper can be used for preliminary architectural acoustic design, especially when designing large auditoriums in which ray acoustics play a dominant role. It is possible to obtain a diffuse sound field by modifying a regular geometry into a chaotic geometry. In room acoustics, designing a ray system with positive Lyapunov exponents may be effective to realize a more uniform sound field. This method is of practical significance to designers in order to gain insight on the dynamics of acoustic rays in enclosed spaces and optimize architectural designs to obtain a satisfactory sound distribution.

Acknowledgments

This work was supported by the National Science Foundation of China (Grant nos.: 11174086 and 1157408). Odeon 12.2 room acoustics software was provided by the Architecture Acoustic Laboratory of the South China University of Technology.

Appendix

Different speakers were used for the room acoustics simulations in this study. The following results show the fluctuations of the SPLs under the excitation of "Danley Sound Labs-SH-25" directional source in the rectangular and concave enclosed spaces with the same dimensions as those used in the simulations based on the "DNH-Tunnel-500" source. These supplementary results support the key findings presented in this paper.

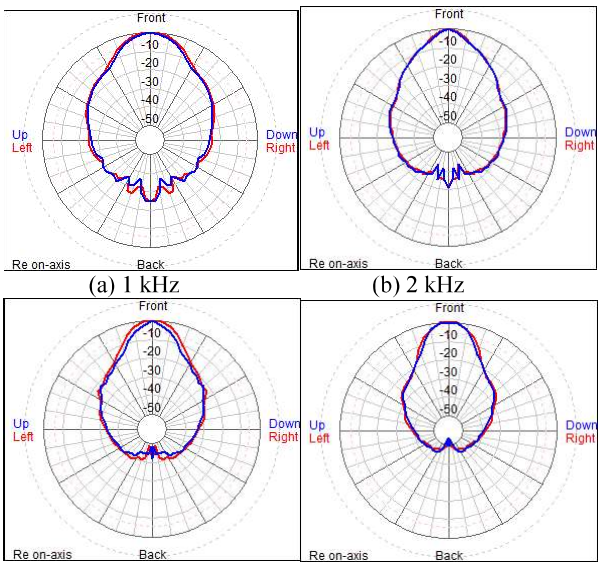

Figure 9: Directivity patterns of the "Danley Sound Labs SH25" source at different frequencies.

Table 3: Uniformity of the sound field under excitation of the "Danley Sound Labs SH25" source.

	1 kHz	2 kHz	4 kHz	8 kHz
	Slope/Sinai	Slope/Sinai	Slope/Sinai	Slope/Sinai
1	101/101.7	98/98.7	96.1/97.1	93.2/94.7
2	101.4/102.8	98.6/100.1	96.6/98.4	93.8/95.8
3	102.3/102.2	99.9/99.3	97.8/97.7	94.8/95.3
4	102.2/102.8	99.7/99.5	97.8/98.3	94.9/96.1
5	102.6/102.9	99.4/99.5	98.0/98.3	95.7/96.1
6	105.1/102.7	101.3/99.1	100.7/98	99.0/95.9
7	100.8/103.0	97.7/99.6	95.9/98.6	93.2/96.5
8	101.3/103.3	98.5/100.0	96.6/98.9	93.8/96.9
9	101.8/103.2	99.2/99.9	97.2/98.8	94.4/96.8
10	102.0/102.8	99.4/99.6	97.5/98.3	94.7/96.1
11	102.7/102.4	99.6/99.0	98.2/97.7	95.9/95.5
12	104.3/102.7	100.7/99.2	99.9/98.0	98.0/95.9
13	101.7/103.0	98.9/99.7	97.1/98.5	94.4/96.3
14	102.1/103.3	99.3/100.2	97.5/98.9	94.8/96.6
15	102.0/103.4	99.3/100.1	97.5/98.9	94.8/96.7
16	102.8/102.7	99.7/99.2	98.3/98.1	96.0/96.0
17	105.1/103.2	101.4/99.6	100.8/98.6	99.0/96.6
18	102.4/102.6	99.6/99.2	98.0/98.0	95.4/95.9
19	102.7/102.7	99.8/99.2	98.2/98.1	95.8/96.0
20	105.3/102.7	101.7/99.3	101/98.2	99.2/96.1
Range	4.5/1.7	4/1.5	5.1/1.8	6/2.2
Variance	1.8090/0.1626	1.1150/0.1674	2.2161/0.2138	3.4846/0.2830

References

[1] H.J. Stöckmann and J. Stein. ''Quantum'' chaos in billiards studied by microwave absorption. *Phys. Rev. Lett.*, 64(19): 2215, 1990.

[2] J. Stein and H.J. Stöckmann. Experimental determination of billiard wave functions. *Phys. Rev. Lett.*, 68(19): 2867, 1992.

[3] M.C. Gutzwiller. Chaos in classical and quantum mechanics. Springer-Verlag, New York, 1990.

[4] K. Nakamura, Quantum chaos: A new paradigm of nonlinear dynamics, Cambridge University Press, Cambridge, 1993.

[5] R. Blümel and W.P. Reinhardt, Chaos in atomic physics, Cambridge University Press, Cambridge, 1997.

[6] X. Lin, Y. Zhang, and G. Du. Influence of perturbations on chaotic behavior of the parabolic ray system. *J. Acoust. Soc. Am.*, 105 (4): 2142, 1999.

[7] M.G. Brown, J.A. Colosi, S. Tomsovic, A. Virovlyansky, M.A. Wolfson, and G.M. Zaslavsky, Ray dynamics in long-range deep ocean sound propagation. *J. Acoust. Soc. Am*, 113(5), 2533, 2003.

[8] D.V. Makarov, M.Y. Uleysky, and S.V. Prants, Ray chaos and ray clustering in an ocean waveguide. *Chaos: Interdiscip. J. Nonlinear Sci.*, 14(1) :79, 2004.

[9] Y. Zhang and X. Xu. Influence of ocean bottom reflection on ray chaotic behaviors in underwater acoustics. *Acta Acust.*, 36(2): 221, 2011.

[10] T. Kawabe, K. Aono, and M. Shin-ya. Acoustic ray chaos and billiard system in Hamiltonian formalism (L). *J. Acoust. Soc. Am.*, 113(2): 701, 2003.

[11] S. Koyanagi, T. Nakano, and T. Kawabe. Application of Hamiltonian of ray motion to room acoustics. *J. Acoust. Soc. Am.*, 124(2): 719, 2008.

[12] X. Yu and Y. Zhang. Acoustic ray diffuse behaviors of an architectural semi-stadium model. *Int. J. Model. Simul.*, 31(4): 301, 2011.

[13] X. Yu and Y. Zhang. Ray chaos in an architectural acoustic semi-stadium system. *Chaos: Interdiscip. J. Nonlinear Sci.*, 23(1): 013107, 2013.

[14] W.J. Cavanaugh and J.A. Wilkes. Architectural acoustics: principles and practice, John Wiley & Sons, Inc., New York, 1999.

[15] H.D.I. Abarbanel, R. Brown, and M.B. Kennel. Lyapunov exponents in chaotic systems: their importance and their evaluation using observed data. *Int. J. Mod. Phys. B*, 5(9): 1347, 1991.

[16] W.B. Joyce. Erratum: Sabine's reverberation time and ergodic auditoriums. *J. Acoust. Soc. Am.*, 59(1): 234, 1976. 58(3) (1975) 643-655.

[17] A. Kulowski. Remarks on a limit value of the sound directional diffusion coefficient in rooms. *Appl. Acoust.*, 32(2): 93, 1991.

[18] B.N. Gover, J.G. Ryan, and M.R. Stinson. Measurements of directional properties of reverberant sound fields in rooms using a spherical microphone array. *J. Acoust. Soc. Am.*, 116(4): 2138, 2004.

[19] T.J. Schultz. Acoustic wattmeter. *J. Acoust. Soc. Am.*, 28(4): 693, 1956.

[20] S.J. Loutridis. Quantifying sound-field diffuseness in small rooms using multifractals. *J. Acoust. Soc. Am.*, 125(3): 1498, 2009.

[21] L.M. Wang and M.C. Vigeant: Evaluations of output from room acoustic computer modeling and auralization due to different sound source directionalities. *Appl. Acoust.*, 69(12): 1281, 2008.

[22] J. Keränen, and V. Hongisto. Comparison of simple room acoustic models used for industrial spaces. *Acta Acust. united with Acust.*, 96(1): 179, 2010.

[23] CLF Group, Common Loudspeaker Format, <http://www.clfgroup.org/files/index.php>, 2018.

[24] T. Papenbrock. Numerical study of a three-dimensional generalized stadium billiard. *Phys. Rev. E*, 61(4): 4626, 2000.